

A 245 GHz LNA in SiGe Technology

Klaus Schmalz, Johannes Borngräber, Yanfei Mao, Holger Rucker, and Rainer Weber

Abstract—A five-stage differential SiGe low noise amplifier (LNA) in cascode topology is presented. Transformer coupling is used between the stages to obtain inter-stage matching. The single ended input and output of the LNA are realized by baluns. The LNA has 18 dB of gain at 245 GHz and a 3 dB bandwidth of 8 GHz. A noise figure of 11 ± 1 dB NF of the LNA at 245 GHz was measured by the Y-factor method. These values represent the highest gain and the lowest measured noise figure at 245 GHz reported for a SiGe LNA so far. The LNA draws 82 mA at a supply voltage of 3.7 V.

Index Terms—Low noise amplifier (LNA), mm-wave circuit, SiGe.

I. INTRODUCTION

THE ISM band at 245 GHz with 2 GHz bandwidth could be used for short-range distance sensor applications. A distance sensor for up to 2 m was previously reported for the 122.5 GHz ISM band with 1 GHz bandwidth [1]. The receiver showed a noise figure (NF) of about 15 dB [1]. Advanced SiGe HBTs with maximum oscillation frequencies f_{\max} in the range of 500 GHz make the 245 GHz ISM band accessible for SiGe BiCMOS technology [2]. Key circuits have been already demonstrated for the frequency range above 200 GHz, e.g., [3]. The low noise amplifier (LNA) is the key building block for a receiver as it strongly influences the NF of the receiver. Effort is therefore needed to get the required LNA performance. A SiGe LNA with three cascaded differential cascode stages was published [3], which showed 15 dB measured gain at 210 GHz and 13 dB simulated NF. A 245 GHz LNA in common base topology was presented [4], which reveals 12 dB measured gain at 245 GHz and 11 dB simulated NF.

This letter presents a five-stage differential SiGe LNA for the 245 GHz ISM band. It uses transformer coupling which is beneficial for amplifiers [5]–[7]. The LNA with transformer-coupled stages in cascode topology achieves a maximum gain of 18 dB at 245 GHz and a measured NF of 11 ± 1 dB.

II. TECHNOLOGY

The circuits were fabricated in a new generation of IHP's 0.13 μm SiGe BiCMOS technology [2]. It features f_T/f_{\max} values of 300 GHz/500 GHz, BV_{CEO} of 1.6 V, a current gain

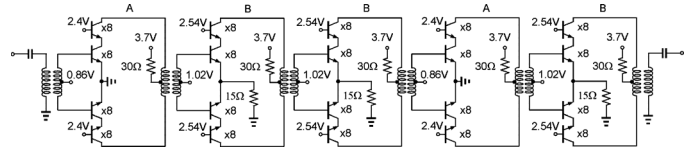


Fig. 1. Schematic of the five-stage 245 GHz LNA.

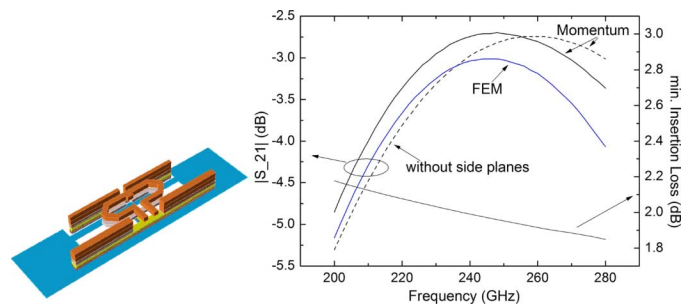


Fig. 2. Layout of the transformer used for EM-simulation, and simulated $|S_{21}|$ and IL_{\min} for $C = 10$ fF at input and output.

of 700, and CML ring oscillator gate delays of 2.0 ps. The back-end-of-line provides five fine-structured aluminum layers, two thick aluminum layers (2 μm and 3 μm thick), and MIM capacitors with 1.5 fF/ μm^2 .

III. CIRCUIT DESIGN

The LNA is a five-stage design with amplifier stages A and B, which are coupled by identical transformers, and baluns at the input and output, respectively, as shown schematically in Fig. 1. The bias points of the amplifier stages are given. Each stage contains four HBTs with $A_E = 8 \times (0.12 \times 0.96) \mu\text{m}^2$ [2]. The simulated NFmin of this HBT is 6 dB at 245 GHz, and the simulated MAG and MSG are 10 dB and 8 dB, respectively. We used weak emitter degeneration in the three B stages to ensure stability of the 245 GHz LNA.

The LNA was designed and tested also as a four-stage LNA, a three-stage LNA, and a two-stage LNA. We applied the design methodology for transformer-coupled cascode topology as described in [7]. The transformer-coupled LNA stage was designed using GoldenGate RF and ADS from Agilent. The transformer and the baluns were simulated with a 2.5D planar EM-simulator (Momentum, Agilent). For the transformer and the baluns we applied S-parameter based models. Fig. 2 shows the simplified layout of the transformer as used for the EM-simulations. It depicts also $|S_{21}|$ and minimum insertion loss of the transformer for the case that maximum $|S_{21}|$ is tuned to 245 GHz by $C = 10$ fF at the input and output. A loss of 2 dB is estimated at 245 GHz. The Momentum results are in reasonable agreement with 3D EM-simulations (FEM, Agilent). The transformer is implemented using the two top metal layers. The

Manuscript received August 17, 2012; accepted August 27, 2012. Date of publication September 20, 2012; date of current version October 03, 2012. This work was supported in part by Land Brandenburg under the project Tele-Diagnostik.

K. Schmalz, J. Borngräber, Y. Mao, and H. Rucker are with the IHP, Frankfurt D-15236, Germany (e-mail: schmalz@ihp-microelectronics.com).

R. Weber is with Fraunhofer IAF, Freiburg D-79108, Germany (e-mail: Rainer.Weber@iaf.fraunhofer.de).

Color versions of one or more of the figures in this letter are available online at <http://ieeexplore.ieee.org>.

Digital Object Identifier 10.1109/LMWC.2012.2218097

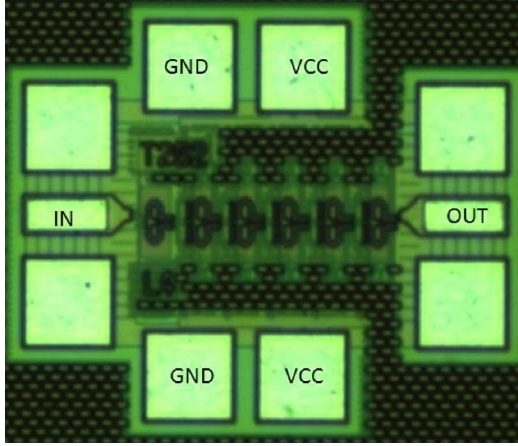


Fig. 3. Chip photo of the five-stage LNA.

primary winding uses the $2\ \mu\text{m}$ thick layer, and the secondary winding uses the $3\ \mu\text{m}$ layer. The input of the primary winding is connected to two metal layer stacks, which are connected to the HBT's collectors in the LNA stage. The middle tap of the primary winding is connected to the VCC metal line with metal layer stacks on both sides. The significant parasitic coupling between the transformer windings and the metal layer stacks is considered in our EM model of the transformer. Due to this coupling the maximum $|S_{21}|$ is shifted to lower frequency compared to the transformer without side planes, see Fig. 2.

The five-stage LNA draws 82.1 mA at 3.7 V supply voltage. Fig. 3 shows the chip photo of the five-stage LNA. The chip size is $0.36 \times 0.43\ \text{mm}^2$, including all pads.

IV. MEASUREMENT RESULTS

The noise figure of the LNA has been calculated with the Y-factor method from on-wafer measurements of the noise power at the output of the LNA, when its input is terminated with a hot and a cold load. The hot load is realized with an RF absorber material at room temperature and for the cold load the absorber is cooled down to 77 K with liquid nitrogen. Fig. 4 shows the setup for the on-wafer noise figure measurement. An H-band horn antenna, which looked alternately on the hot and cold RF absorber material, has been mounted at the Cascade Microtech i325-S infinity probe tip at the input. The output signal of the LNA is amplified with an H-band LNA module and down-converted with a sub-harmonically driven H-band receiver to the IF input of the Agilent N8975A noise figure analyzer (NFA). At each frequency point the NFA measures the noise power of the LNA for the hot and cold absorber material. Indeed, the cold temperature at the LNAs input rises to 187 K due to the 3.0 dB loss of the probe tip [8]. The ratio of the hot and the cold noise power is the Y factor. Together with the excess noise ratio (ENR), which is the ratio of the difference of the hot and cold temperature to the reference temperature $T_0 = 290\ \text{K}$, the noise figure of the MMIC can be calculated [9]. Because the NFA measures absolute values more than one measurement should be used to minimize the measurement's error of the DUT's noise figure.

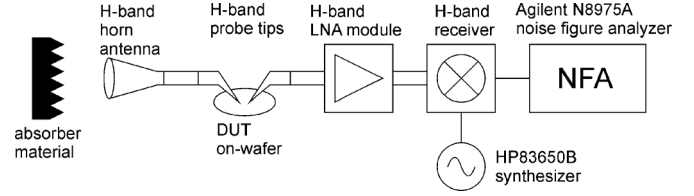


Fig. 4. Setup for noise figure measurement.

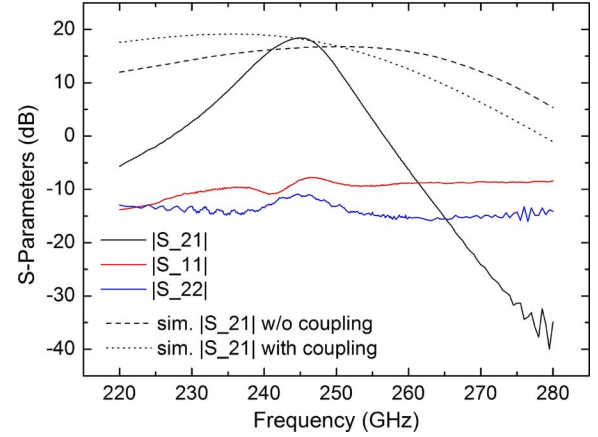


Fig. 5. Measured and simulated gain curves for five-stage LNA, and measured input and output losses.

Fig. 5 presents the measured gain ($|S_{21}|$) of the five-stage LNA together with simulated gain and the input and output return losses ($|S_{11}|$ and $|S_{22}|$). $|S_{11}|$ is higher than $-8\ \text{dB}$ in the range 220 – 330 GHz, and $|S_{22}|$ is $-11\ \text{dB}$ at 245 GHz, indicating that increased LNA gain is possible by optimized matching. The five-stage amplifier demonstrates 18.4 dB maximum gain at 244.5 GHz. The simulated maximum gain of the five-stage LNA at 245 GHz is close to the measured gain value, but the pronounced band-pass gain curve is not revealed by the simulations. We performed simulations (i) with identical S-parameter based transformer models for each LNA stage, and (ii) with an S-parameter based model for all transformers including coupling between the transformers. This coupling effect leads to decreased gain at frequencies beyond 260 GHz compared to case (i), but the measured gain decreases considerably stronger. We assume that the observed narrow band-pass gain curve is related to parasitic effects in the HBT cascode stage, which are not considered in our simplified transformer model.

To analyze the stability of LNA, we simulated the μ -factor, which is sufficient to determine unconditional stability. The μ -factors for the five-stage LNA, and the LNA stages A and B, respectively, have indicated unconditional stability for the five-stage LNA. Fig. 6 shows the measured gain $|S_{21}|$ for LNAs with four stages, three stages, and two stages, respectively, and the simulated $|S_{21}|$ for the two-stage LNA. Compared to the 18.4 dB gain of the five-stage LNA, see Fig. 5, the four-stage LNA shows 12.6 dB gain at 245.4 GHz. The three-stage LNA has 6.5 dB gain at 243.3 GHz, and the two-stage LNA demonstrates 1.2 dB gain at 243.6 GHz. The simulated maximum gain of the two-stage LNA is 2.7 dB. From the measured gain one can see that each single LNA stage achieves a gain of about 6 dB when implemented in the chain.

TABLE I
COMPARISON OF MM-WAVE LNAs

	Freq. (GHz)	f _T /f _{max} (GHz)		Stages	Gain (dB)	NF (dB)	DC power	Area (mm ²)
Öjeförs [3]	210	280/435	SiGe	3, differ.	14	13 (sim.)	42mA @ 3.6V	
Mao [4]	245	300/500	SiGe	4	12	11.3 (sim.)	14mA @ 2V	0.42 x 0.46
Gaier [8]	270		InP HEMT	3	11.4	7.5	13.9mA @ 0.8V	0.65 x 0.43
Tessmann [10]	320	380	mHEMT	4	19.5	7.3 (sim.)	45mA @ 2V	0.5 x 1.2
Deal [11]	670 660	1200/>600	InP HEMT	5 10	11-12 30	13 (meas.)		0.655 x 0.375 0.655 x 0.375
Deal [12]	480	1200/580	InP HEMT	5	11.7			0.9x0.32
This work	245	300/500	SiGe	5, differ.	18	11±1 (meas.)	82mA @ 3.7V	0.36 x 0.43

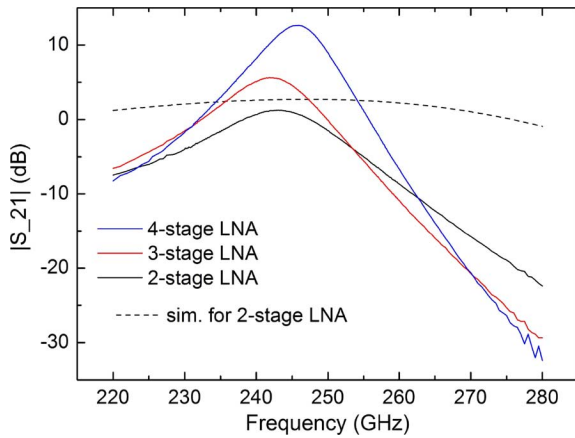


Fig. 6. Measured and simulated gain curves for two-stage LNA, and measured gain curves for the three- and four-stage LNA, respectively.

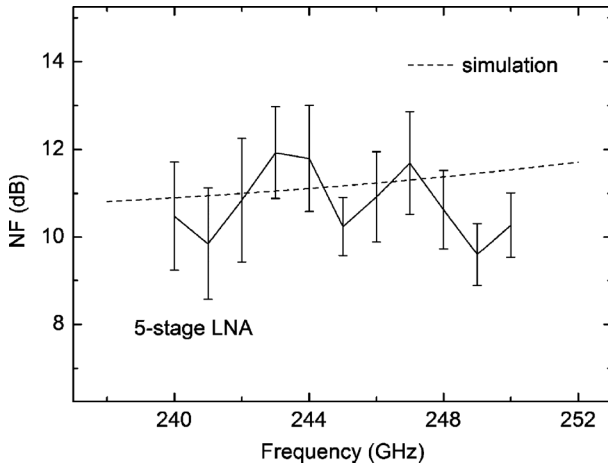


Fig. 7. Measured and simulated NF for the five-stage LNA.

Fig. 7 presents the measured NF of the five-stage LNA for the frequency range 240 – 250 GHz. The NF values with their standard errors were obtained by averaging five data sets. The simulated NF curve is close to the measured NF values. The higher NF compared to NF_{min} (6 dB) of the transistor is due to the cascode transistors in the first stage, noise contributions from the second stage, and the loss of the input balun.

Table I compares the results of this letter with previous work [10]–[12].

V. CONCLUSION

In this letter, we reported a 245 GHz five-stage differential LNA in cascode topology with transformer coupling between the stages using high-performance SiGe BiCMOS technology. A measured gain of 18 dB and a measured noise figure of 11 ± 1 dB have been achieved at 245 GHz. To the best of our knowledge, this is the highest gain and the lowest measured NF at 245 GHz reported for a SiGe LNA so far.

REFERENCES

- [1] I. Sarkas, J. Hasch, A. Balteanu, and S. P. Voinigescu, "A fundamental frequency 120-GHz SiGe BiCMOS distance sensor with integrated antenna," *IEEE Trans. Microw. Theory Tech.*, vol. 60, no. 3, pp. 795–812, Mar. 2012.
- [2] H. Rücker, B. Heinemann, and A. Fox, "Half-terahertz SiGe BiCMOS technology," in *IEEE SiRF Symp. Dig.*, Jan. 2012, pp. 129–132.
- [3] E. Öjeförs, B. Heinemann, and U. Pfeiffer, "Subharmonic 220- and 320-GHz SiGe HBT receiver front-ends," *IEEE Trans. Microw. Theory Tech.*, vol. 60, no. 5, pp. 1397–1404, May 2012.
- [4] Y. Mao, K. Schmalz, J. Borngräber, and J. C. Scheytt, "A 245 GHz CB LNA in SiGe," in *Proc. Eur. Microw. Integr. Circuits Conf. (EuMIC)*, Oct. 2011, pp. 224–227.
- [5] Z. Xu, Q. J. Gu, and M.-C. F. Chang, "A three stage, fully differential 128–157 GHz CMOS amplifier with wide band matching," *IEEE Microw. Compon. Lett.*, vol. 21, no. 10, pp. 550–552, Oct. 2011.
- [6] Z. Xu, Q. J. Gu, and M.-C. F. Chang, "A 100–117 GHz W-band CMOS power amplifier with on-chip adaptive biasing," *IEEE Microw. Compon. Lett.*, vol. 21, no. 10, pp. 547–549, 2011.
- [7] A. Arabian, S. Callender, S. Kang, B. Afshar, J.-C. Chien, and A. M. Niknejad, "A 90 GHz-carrier 30 GHz-bandwidth hybrid switching transmitter with integrated antenna," in *IEEE ISSCC Symp. Dig.*, Feb. 2010, pp. 12–14.
- [8] T. Gaier, L. Samoska, A. Fung, W. R. Deal, V. Radisic, X. B. Mei, W. Yoshida, P. H. Lui, J. Uyeda, M. Barsky, and R. Lai, "Measurement of a 270 GHz low noise amplifier with 7.5 dB noise figure," *IEEE Microw. Wireless Compon. Lett.*, vol. 17, no. 7, pp. 546–548, Jul. 2007.
- [9] Agilent, "Fundamentals of RF and Microwave Noise Figure Measurements," Appl. Note 57-1, 2012 [Online]. Available: <http://cp.literature.agilent.com/litweb/pdf/5952-8255E.pdf>
- [10] A. Tessmann, A. Leuther, H. Massler, M. Kuri, M. Zink, M. Riessle, and R. Lösch, "High-gain submillimeter-wave mHEMT amplifier MMICs," in *Proc. IEEE Int. Microw. Symp. (IMS)*, May 2011, pp. 53–56.
- [11] W. R. Deal, K. Leong, V. Radisic, S. Sarkozy, B. Gorospe, J. Lee, P. H. Liu, W. Yoshida, J. Zhou, M. Lange, R. Lai, and X. B. Mei, "Low noise amplification at 0.67 THz using 30 nm InP HEMTs," *IEEE Microw. Compon. Lett.*, vol. 21, no. 7, pp. 368–370, Jul. 2011.
- [12] W. R. Deal, X. B. Mei, V. Radisic, K. Leong, S. Sarkozy, B. Gorospe, J. Lee, P. H. Liu, W. Yoshida, J. Zhou, M. Lange, J. Uyeda, and R. Lai, "Demonstration of a 0.48 THz amplifier module using InP HEMT transistors," *IEEE Microw. Compon. Lett.*, vol. 20, no. 5, pp. 289–291, May 2010.